J. Physiol. (1981), **313**, *pp.* 415–437
With 12 text-figures
Printed in Great Britain

EVIDENCE FOR THE PRESENCE OF POTASSIUM CHANNELS IN THE PARANODAL REGION OF ACUTELY DEMYELINATED MAMMALIAN SINGLE NERVE FIBRES

BY S. Y. CHIU AND J. M. RITCHIE

From the Department of Pharmacology, Yale University School of Medicine, New Haven, Connecticut 06510, U.S.A.

(*Received 4 June 1980*)

SUMMARY

1. A study has been made of the ionic currents in voltage-clamped single rabbit nodes of Ranvier at 22–26 °C both under normal conditions, and after the nerve fibres had been acutely demyelinated by a variety of treatments designed to loosen the myelin from the axonal membrane.

2. The myelin-loosening treatments included application of various combinations of: lysolecithin (to dissolve the myelin); collagenase (to loosen the connective tissue in the nodal region); high-potassium Locke solution, hypertonic and hypotonic solutions (to induce axonal volume changes).

3. At a critical stage in such treatment (usually after 15–45 min) a large outward current suddenly appeared.

4. There was no substantial change in the size of the measured inward sodium current when measured at this critical stage.

5. The outward current was blocked by internal TEA and caesium ions, had a reversal potential that became more positive when the external potassium concentration was increased, was kinetically similar to the known potassium current in frog fibres, and was therefore assumed to be a potassium current.

6. The phase of large outward current, whenever it appeared, was always accompanied by the appearance of a slow transient capacitative component in the leakage current, which indicated a marked increase in the effective nodal capacity (of 10- to 60-fold). We suggest that the slow transient capacity current reflected charging of newly exposed axonal membrane, probably in the paranodal region, which was uncovered by the various acute demyelination treatments. This internodal membrane seems to contain mostly potassium channels and few, if any, sodium channels.

7. Newly dissected fibres occasionally showed large potassium currents before treatment, particularly if they were deliberately stretched during dissection; a marked slow capacity transient current was consistently present in these fibres.

8. The effects of acute paranodal demyelination on the sodium and potassium currents, and on the transient capacity currents, can be simulated by a model in which the node is coupled to a cable-like paranode which contains Hodgkin–Huxley type potassium channels and which has a much higher leakage resistance.

0022-3751/81/4190-1005 $07.50

9. The functional significance of the presence of potassium channels in the internodal region (at least in the paranode) of mammalian fibres is discussed.

INTRODUCTION

Chiu, Ritchie, Rogart & Stagg (1979) and Brismar (1979, 1980) have recently confirmed the original observation of Horackova, Nonner & Stämpfli (1968) that the phase of later outward current carried by potassium ions in frog and squid nerve is virtually absent in voltage-clamped mammalian nodes of Ranvier, suggesting that the nodal membrane in the mammal generally has few, if any, potassium channels. However, several pathophysiological findings suggest that mammalian nerve does not absolutely lack the ability to generate potassium currents. For example, Brismar (1979) has demonstrated in myelinated nerve fibres from alloxan diabetic rats the presence of a large outward potassium current; such current is small in normal fibres. Since diabetic neuropathy in man is characterized by segmental demyelination, a possible explanation of this finding is that in the alloxan diabetic rat the normal close contact between the Schwann cell and the axonal membrane has been so disrupted as to uncover membrane, and hence potassium channels, in the paranodal region normally covered by myelin. Secondly, it has been shown by Sherratt, Bostock & Sears (1980) that continuous conduction can occur in rat demyelinated nerve fibres, and that TEA and 4-aminopyridine, which are known to block potassium channels, prolong the action potentials in this situation. This sensitivity to TEA and 4-aminopyridine again suggests that the axonal membrane exposed by the demyelination possesses potassium channels. Furthermore, H. Bostock & M. E. Smith (unpublished observations) have shown that within 2 days of exposure to lysolecithin, some rat nodes exhibit a phase of outward current that is sensitive to 4-aminopyridine. Finally, large potassium currents are occasionally found in apparently normal mammalian nodes, which might reflect mechanical stretching of the node during dissection. These experiments suggest either that chronic disruption of the myelin somehow, in time, induces formation of new potassium channels in the internodal axonal membrane, or that potassium channels are normally present, but hidden, under the myelin. Support for the latter possibility is provided in the present voltage-clamp experiments on acutely demyelinated rabbit nodes (see also Chiu & Ritchie, 1980*a*, *b*).

METHODS

Single myelinated fibres from rabbit sciatic nerves were dissected and voltage-clamped at 22–26 °C as described previously (Chiu *et al.* 1979; Chiu, 1980). The holding potential was then adjusted to give a resting inactivation of about 0·25 ($h_\infty = 0{\cdot}75$), and the corresponding absolute membrane potential was assumed, on the basis of the arguments presents by Chiu *et al.* (1979), to be −80 mV. The main experimental protocol involved the measurement of the nodal current-volage relationship before and after treatment designed to loosen the myelin in the paranodal region (see below). The generation of the command pulse sequence for this measurement, and the storage of the current responses in the computer, have been described previously (Chiu, 1980).

Solutions. Normal Locke solution for the rabbit node contained (mM): NaCl, 154; $CaCl_2$; 2·2; KCl, 5·6; and morpholinopropionyl sulphonate buffer (pH 7·4), 10. Unless otherwise mentioned, the ends of the fibres were cut in 160 mM-KCl (present in the two end-pools).

Myelin-loosening treatment. Two types of treatment, one chemical and the other osmotic, were used to disrupt the myelin investing the paranodal region. The chemical treatment involved

perfusing the node while in the chamber for voltage-clamping with a Locke solution containing 0·1–0·2 % lysolecithin, an agent known to cause demyelination through its detergent action (Hall, 1972; Smith & Benjamins, 1977). In earlier experiments, the fibre was sometimes first treated with collagenase (Sigma, 10–20 μg/ml.) for about 5 min before application of the lysolecithin. The osmotic treatment, usually applied immediately after lysolecithin, involved alternating the solution bathing the node between normal Locke solution and various modified Locke solutions either with elevated potassium (80 mM) or of abnormal tonicity to produce acute volume changes in the nerve. Hypertonic solutions were prepared by addition of 0·5 M-sucrose to Locke solution, and hypotonic solutions by diluting Locke solution with an equal amount of water. During treatment the nodal currents were checked periodically for any increase in the late outward current. Any late outward current that was present initially was always very small and usually remained constant. This situation persisited for the first 15–45 min of treatment, when a dramatic large phase of outward current often suddenly appeared. When this was observed, the node was quickly washed with fresh normal Locke solution and the electrical measurements were resumed. If the treatment did not result in a significant increase in the late current after about an hour, the experiment was terminated; the fibre at this time usually displayed signs of deterioration, the sodium currents decreasing, and the leak current greatly increasing.

Measurement of the nodal capacity. A value for the apparent nodal capacity was calculated from a current response associated with a hyperpolarization to −125 mV. From such records (Fig. 12*Ab*, *Bb*), a leakage component L was first subtracted, and the remaining current, assumed to be entirely capacity current, was integrated numerically to obtain the associated charge. The capacity current generally declined in an initial fast phase followed by a slow phase. The slow phase was usually small or neglible in most normal nodes (Fig. 12*Ab*); but it was much more prominent in nodes after myelin-loosening treatment (Fig. 12*Bb*). Whenever such a slow capacity transient could be resolved, the leakage component L was obtained by fitting the slow declining portion of the hyperpolarizing current response, by an equation of the form

$$y = A \exp(-t/\tau_s) + L \tag{1}$$

The associated capacity charge was calculated as:

$$Q_c = \int_0^{t_0} (I - L) \cdot dt + \int_{t_0}^{\infty} A \exp(-t/\tau_s) \cdot dt, \tag{2}$$

where t_0 denotes the end of the hyperpolarizing pulse, A is the size of the current at this time, and I is the current in response to the hyperpolarization. In the normal node the value of Q_c is determined by the first integral (which reflects both fast and slow current transients) whereas the second integral contributes only to a minor extent to the value of Q_c. The capacity was then calculated by dividing Q_c by the size of the hyperpolarizing pulse, which was typically 45 mV.

Time constant of the late current. A value for the time constant of the late current, τ_n, was calculated from the data record by first determining I_0 in eqn. (3) (p. 9), taken to be the size of the late current at the end of the test pulse (i.e. after 4–8 msec), and then normalizing the entire late current with respect to I_0. By taking the fourth root of this normalized current and subtracting unity from it, we obtained a hypothetical declining current corresponding to the term $\exp[t_D - t)/\tau_n]$ in eqn. (3); t_D is an arbitrary delay of 100–500 μsec (as in Cole & Moore, 1960, and more recently in Keynes & Kimura, 1980). This current was found to decline more or less with a single exponential to about 80 % completion; thereafter it declined 5–10 times more slowly. Ignoring this second slow decline, we fitted the initial 70–80 % of the decline to the expression $\exp[(t_D - t)/\tau_n]$ using a programme described previously (Chiu, 1980).

Whenever possible mean values ± their standard errors are quoted.

RESULTS

The main result in the present study is that large voltage-sensitive outward currents can be produced in voltage-clamped rabbit nodes by treatment likely to lead to mechanical or chemical disruption of the myelin in the paranodal region. The following sections first describe the experimental conditions for this to occur; then

evidence is produced that suggests that the late current found under these conditions is a potassium current; and finally, a hypothesis is put forward to explain these observations.

Treatment leading to dramatic increase in late outward current in rabbit node

Records of the ionic currents were obtained first in a normal voltage-clamped rabbit node of Ranvier. Little or no outward current was found (Horackova *et al.* 1968; Chiu *et al.* 1979; Brismar, 1980); and such outward current as was present was quite

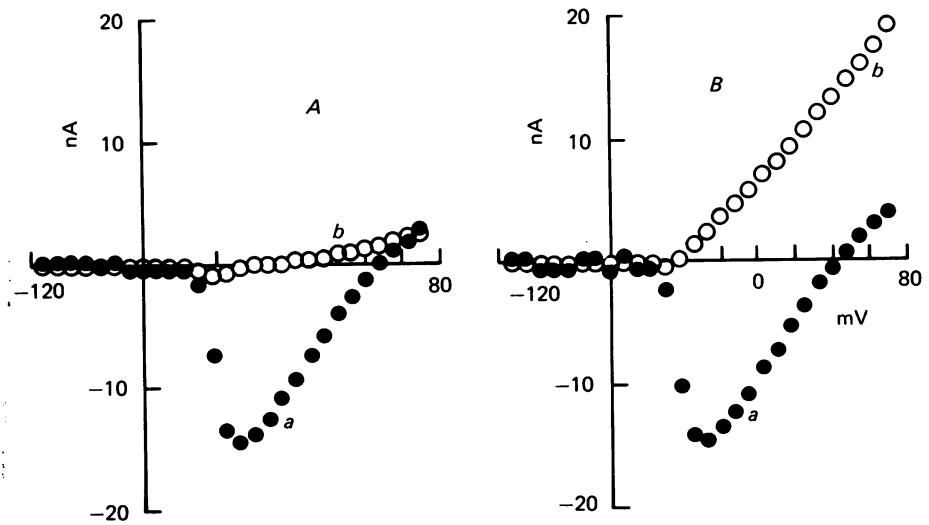

Fig. 1. Current–voltage relations of the early inward and late outward currents before and after myelin-loosening treatment in a rabbit sciatic node. *a*, peak of early inward sodium current. *b*, late outward current measured 4 msec after onset of the test pulse after subtraction of a linear leakage current. Same fibre as in Fig. 1.

insensitive to externally applied TEA (Chiu & Ritchie, 1980). The node was then subjected to one of the treatments described above in an attempt to disrupt the myelin from the paranodal region. In our earlier experiments the node was first exposed to collagenase (about 10 μg/ml.) for about 5 min, followed by an alternation of the bathing solution of the node (4 times, 2–5 min) between normal Locke solution and a modified Locke solution in which half of the sodium was replaced by potassium. Since high potassium-Locke solution causes muscle cells to swell (Hodgkin & Horowicz, 1959; Mobley & Page, 1971), this procedure might be expected to cause the nerve volume or the myelin to expand and contract sequentially, tending to detach the myelin from the axon in the paranodal region. During the first 15–45 min of treatment, the early sodium current often decreased (but only slightly) presumably because of the fibre running down. Furthermore, during this time any late outward current that was present remained very small and exhibited practically no change. Then, suddenly, over a period of about 3 min, the late outward current underwent a dramatic increase (as in Fig. 12*Ba*). After this had happened, the fibres tended to deteriorate quickly, although some fibres were sufficiently stable to allow testing the

effect of various changes of the bathing solution. The late outward current was unaffected by TTX whereas the early inward current was completely abolished (Chiu & Ritchie, 1980*b*).

When the large increase in outward current occurred there was usually no accompanying immediate change in the early sodium current (see, for example, Fig. 12*Aa*, *Ba*) although in two experiments a small increase ($< 5\%$) in the sodium current did occur.

Fig. 1 shows the current–voltage relationships for the early sodium (*a*) and late outward current (*b*) before (*A*) and after (*B*) the myelin-loosening treatment. Clearly, there was little change in the former whereas the latter was markedly changed.

Similar results were obtained if Locke solutions with abnormal tonicity were used instead of high-potassium Locke solution, or if the detergent lysolecithin was used instead of collagenase.

The nature of the late outward current revealed by the treatment

Four lines of evidence, to be discussed below, are consistent with the idea that this late current revealed by the myelin-loosening treatment is kinetically and pharmacologically similar to the potassium current normally present in frog and other nerve, so that part or all of the late current in the present study could be carried by potassium ions. The errors introduced by the acute demyelination in the voltage control and in the kinetics of the late current, which introduce some uncertainty in the analysis, will be examined quantitatively in detail in a subsequent section (p. 431).

Effect of TEA and Cs

First, as described earlier (Chiu & Ritchie, 1980), this outward current was much reduced (by about 70%) when TEA and Cs ions were applied internally by equilibrating the cut ends of the fibre in solutions containing these ions (80 mM-TEA, 80 mM-Cs) and allowing diffusion along the internode to occur (Koppenhöfer & Vogel, 1969). When the TEA ions were applied externally the block was less effective. External application of TEA in concentrations up to 20–60 mM depressed the late current by at most 20–30%, with the block developing very slowly and never becoming complete.

Kinetics

Secondly, the late current in the present study could be reconstructed (see Chiu & Ritchie, 1980) with apparent n^4 kinetics in much the same way as the known potassium current in frog nodes, i.e. the current was of the form

$$I = i_0\{1-\exp[(t_D-t)/\tau_n]\}^4 \qquad (3)$$

with $I = 0$ for $t < t_D$. The voltage dependence of τ_n, obtained from such kinetic reconstruction after lysolecithin treatment was similar to that already found after collagenase treatment (Chiu & Ritchie, 1980*b*), namely τ_n decreased with increasing degrees of depolarization. Near 25 °C the value of τ_n at zero mV is about 0·8–1·0 msec, compared to the corresponding value of 1·5 msec for the potassium current in frog node at the same temperature (Hille, 1971).

Reversal potential

Thirdly, the late outward current exhibited a reversal potential that was sensitive to changes in external potassium concentrations in the way expected of a potassium current. For example, Fig. 2 shows the effect on the late current of increasing the external potassium concentration, $[K]_o$ from 2·5 to 80 mM. The family of late currents

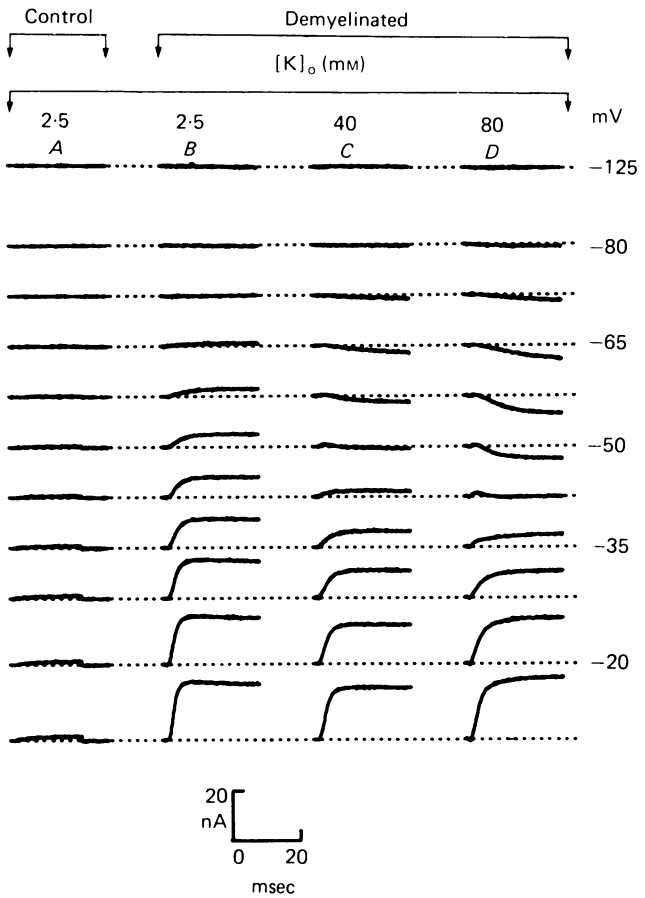

Fig. 2. The effect of changing the external potassium concentration on the late outward current. Each of the four columns of currents (*A*, *B*, *C*, *D*) was generated by the same series of potential changes from an initial value of −80 mV to the potentials indicated on the right. A linear leakage was subtracted, and TTX was used to block the sodium current. *A* shows the control current. *B* shows the late current revealed by treatment with lysolecithin. *C* and *D* show the effects of progressively increasing the external potassium concentration from 2·5 mM in *B* to 40 mM (*C*) and 80 mM (*D*) respectively. Temperature, about 25 °C.

on the left was obtained in $[K]_o = 2·5$ mM with the nodal membrane clamped to a series of increasing potentials. The current was outward for all potentials and no inward current could be resolved. However, when $[K]_o$ was increased to 80 mM the direction of the late current was found to be clearly inward over a small potential range

(−80 to −50 mV) before becoming outward at large depolarizations. The potential at which the late current reversed direction (i.e. the reversal potential) depended on $[K]_o$ as is shown in Fig. 3 in which the steady-state current voltage relationship for the late current is plotted as a function of $[K]_o$.

Clearly, increasing $[K]_o$ made the reversal potential more positive. If all the late current was carried by potassium ions, the theoretical change in the reversal

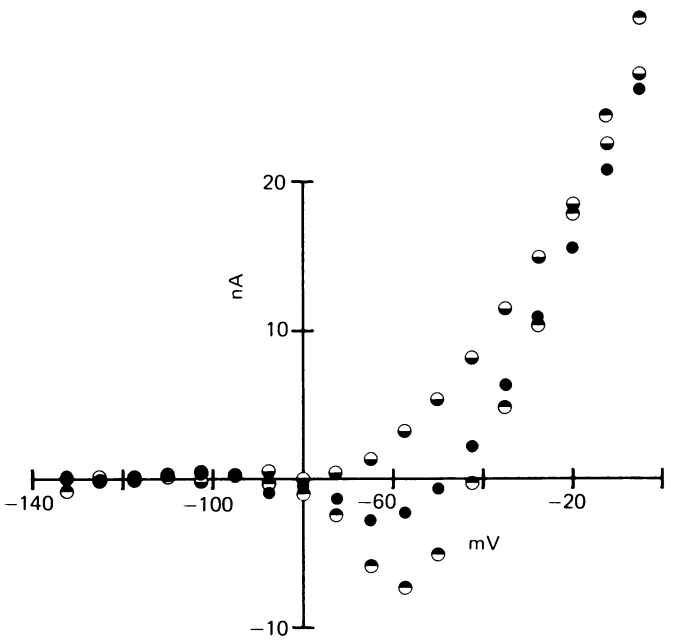

Fig. 3. Current–voltage relationship of the late outward current at different external potassium concentrations (◒, 2·5 mM-K; ●, 40 mM-K; ◓, 80 mM-K). Note that increasing the external potassium concentration made the reversal potential more positive. Same experiment as Fig. 2.

potential, $\triangle E_K$, for a given change in the external potassium concentration would be given by the Nernst equation

$$\triangle E_K = (RT/F) \ln [K]''_o/[K]'_o \tag{4}$$

where $[K]'_o$ and $[K]''_o$ are the two different external potassium concentrations respectively. This equation, however, predicts a bigger change in the reversal potential than was in fact observed. For example, according to Fig. 3, the observed change in the reversal potential was about 10 mV when $[K]_o$ was increased from 40 to 80 mM whereas the corresponding theoretical change calculated with eqn. (4) should have been 18 mV. This discrepancy might be explained if the 'late' channel were not perfectly selective to potassium ions. But it might also reflect uncertainties in measuring the reversal potential due to voltage non-uniformities along a partially demyelinated axon.

Tail currents

Finally, if the delayed response in the fibres subjected to the myelin-loosening treatment were indeed an outward potassium current, then potassium ions might be expected to accumulate in the periaxonal space because of their restricted ability to diffuse into the bulk extracellular fluid (Frankenhaeuser & Hodgkin, 1956). At the end of the depolarizing voltage-clamp pulse, therefore, the resting potential to which

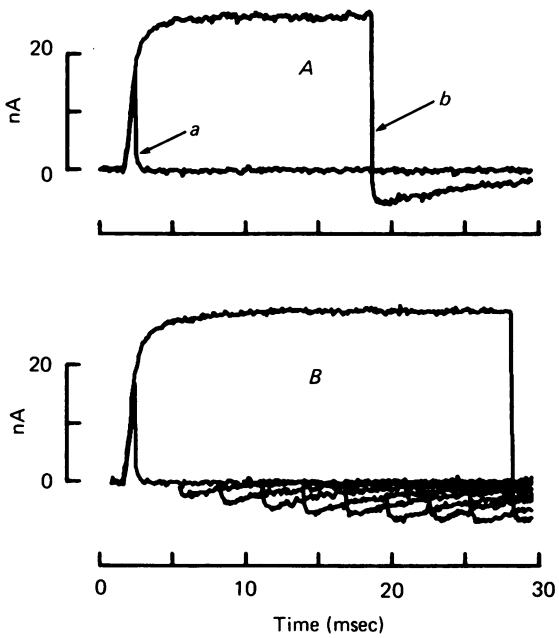

Fig. 4. The effect of the duration of the test-pulse on the tail current following the late outward current. *A* shows two superimposed records for the late current obtained by depolarizing the membrane to +50 mV for 1 msec (*a*) and 17 msec (*b*) before repolarizing the membrane to the original holding potential of −80 mV. Note that the longer depolarization in (*b*) induced an inward tail current when the pulse ended. *B* shows more clearly the development in the size of the inward tail current by superimposing more current records with different pulse durations. Current signals sampled at intervals of 100 μsec throughout.

the fibre returned (−80 mV) may have been considerably more negative than the potassium equilibrium potential because of this periaxonal accumulation of potassium. Until this excess potassium was dissipated by diffusion or reuptake by the fibre, therefore, there would have been a phase of *inward* potassium current. Furthermore, such inward tail currents should be more pronounced the longer the depolarizing voltage-clamp pulse. Fig. 4 shows that this is indeed the case.

Hypothesis for the internodal origin of the potassium current

We conclude from the above pharmacological experiments and the kinetic analysis that the late current revealed by the treatment is not an experimental artifact, but is a voltage-sensitive potassium current similar to that normally present in frog and squid nerve. Where do these potassium currents originate?

An important clue as to the origin of the potassium current is found in a characteristic change in the shape of the capacity transient current that occurred concomitantly with the large increase in the late potassium current. Whereas in the control the initial capacity transient settled quickly in a fraction of a millisecond to a steady leakage value (first few sample points after the pulse in Fig. 12*Ab*), after treatment an additional dominant slower current transient developed with an approximate time constant of 0·5–1·5 msec (Fig. 12*Bb*). This current transient was not affected by TTX or by TEA.

One explanation for the appearance of the slow capacity transient is that the membrane capacity in the treated fibres may be imperfect, as has been discussed by Hodgkin, Huxley & Katz (1952) for the squid giant axon. An alternative explanation, which we believe applies to the node, is that this slow capacity transient current reflected charging of a large amount of newly exposed membrane, probably in the paranodal region, which was uncovered by the myelin-loosening treatment. This explanation is similar to that suggested by Hille (1967) to account for a similar phenomenon in frog nodes after they have been left in the isolated state for several hours, or after poor dissection. For the particular node in Fig. 1 (also Fig. 12), the total capacity (eqn. (2)) increased from an initial value of 2·5 pF to about 35 pF, with the increase coming mainly from the slow capacity current. Interestingly, the increase in both the outward current and the capacity was not accompanied by a corresponding increase in the early sodium current (Fig. 12*Aa*, *Ba*), suggesting that the newly exposed axonal membrane had relatively few sodium channels compared to potassium channels.

In six fibres (of a total of fifteen tested) the effect developed in so similar a fashion that the responses could be averaged. The outward current measured at +70 mV and the associated leakage current for these six fibres are shown in Fig. 5 before and after the increase occurred. For each set of traces (each individual experiment), one pair of currents (*a*) represents the outward currents before treatment (upper of pair, slow capacity current absent) together with the current produced by a hyperpolarizing voltage pulse (lower of pair); the other pair of traces (*b*) are the corresponding currents after treatment (slow capacity current prominent). Clearly, the increase in the late outward current was always accompanied by a corresponding increase in the slow capacity current transient. From each experiment of Fig. 5, a value was calculated for the increase in the capacity (which gives a measure of the apparent increase in axonal membrane area) by integration (for 4–10 msec) of the difference between the pair of capacity transients (after subtraction of a constant leakage as described in the Methods) before and after treatment. For these six fibres, an increase in the late current (measured at +70 mV) of 34·7 ± 3·6 nA from an initial value of 4·9 ± 0·7 nA was associated with a calculated increase in capacity of 86·2 ± 14·4 pF. The early fast capacity transients in the control (first 20–30 μsec) corresponded to a value of 1·4 ± 0·3 pF, which is assumed in this paper to be the capacity of a normal node. The sodium reversal potential, E_{Na}, measured for these six fibres in the control before the increase of the late current, was 52·3 ± 2·7 mV. Whenever measured at the critical moment when the late current increased, no significant change in E_{Na} was observed (Fig. 1). The total steady current–voltage relationships for these six experiments are shown in Fig. 6; as can be seen after treatment the total steady current became markedly rectified with large depolarizations.

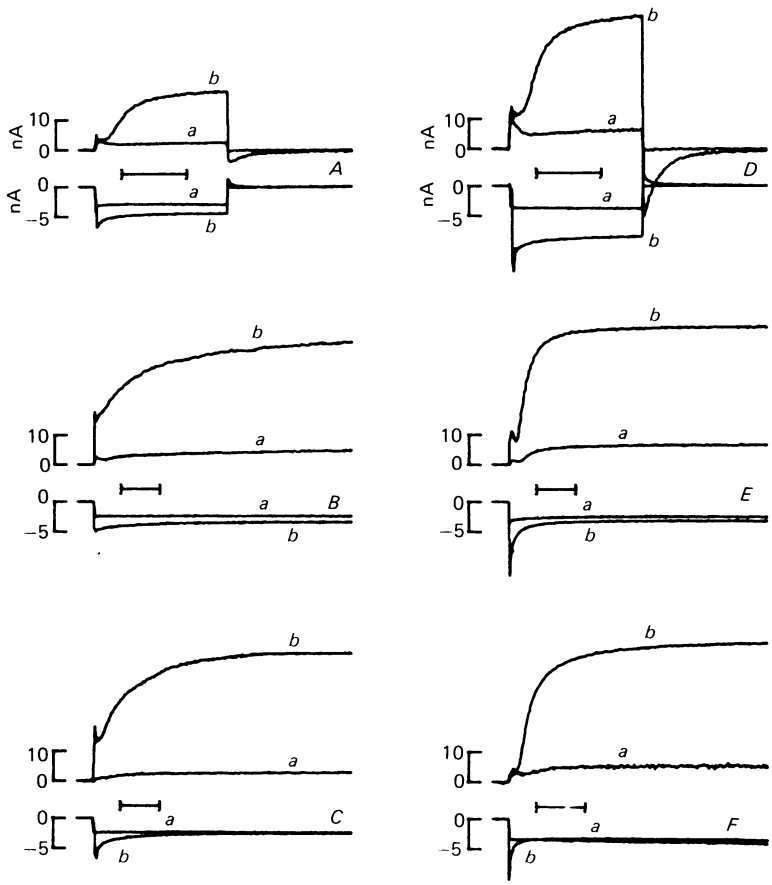

Fig. 5. The effect of the myelin-loosening treatment on the late outward current and on the leakage current in six fibres. Each of the six groups of traces shows two pairs of superimposed records for the late current at +70 mV (upper pair) and the leakage currents (lower pair) before (*a*) and after (*b*) treatment. The type of treatment used was: *A*, collagenase + KCl; *B*, collagenase; *C*, collagenase + KCl; *D*, lysolecithin + KCl; *E*, sucrose; *F*, collagenase + KCl. Note that in each fibre, the marked increase in the late current after treatment is accompanied by the appearance of a large slow capacity current transient that is not prominent in the control leakage current. Only the current signals obtained with sampling intervals ranging 30–50 μsec are shown. Whenever present, the current signals after the pulse were sampled at intervals five times longer than that used during the pulse, and the corresponding time scale was compressed five fold compared to that indicated during the pulse. The horizontal bar in each group of traces corresponds to 2 msec.

Based on the above observations that the outward, putative potassium, current could be selectively increased markedly over the sodium currents by various acute demyelination treatments, we propose that the internodal axon, at least in the paranodal region, normally contains potassium channels and few, if any, sodium channels.

On the basis that in a normal 20 μm diameter fibre the nodal capacity is 1·4 pF,

and that the nodal gap is 2 μm, this hypothesis suggests that the myelin-loosening treatment, which results in an increase in capacity of about 100 pF, would have exposed a length of axon about 150 μm in length (see Fig. 12*Bf*) i.e. the bulk of the paraonodal membrane would be involved.

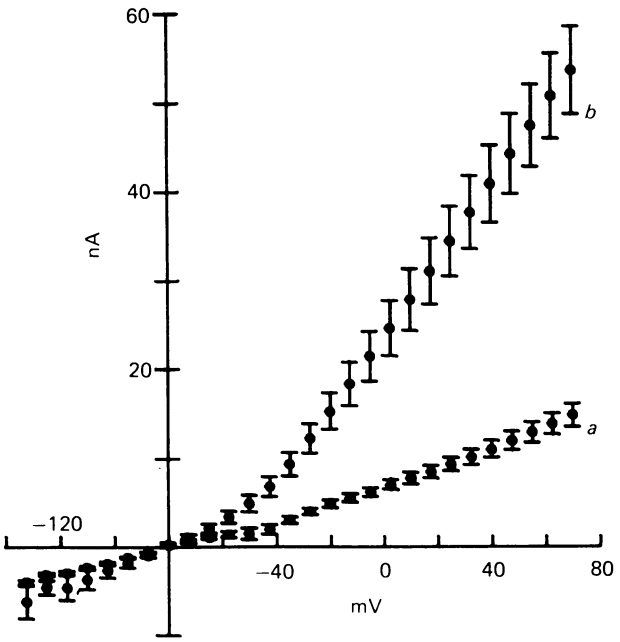

Fig. 6. Current–voltage relationship of the total steady-state membrane current before (*a*) and after (*b*) myelin-loosening treatment. The data (mean values ± 1 S.E.) are from the six rabbit nodes in Fig. 5. The *total* steady currents are measured 4–8 msec after onset of the test pulse. Temperature 24 ± 2 °C.

The linear nature of the capacity

Membrane currents were measured in response to a series of increasing hyperpolarizing pulses applied from a holding potential of −80 mV. The charge carried by the slow capacitative transient during the pulse, which was obtained by integrating the hyperpolarizing current response after subtracting a steady-state value, was then compared with that obtained after the pulse. Such an integration, shown in the right of Fig. 7 for the various hyperpolarizations, shows clearly that the charge that moved during the slow current transient during the pulse returned almost entirely when the pulse ended. Furthermore, the slow current behaved linearly with voltage, as is shown in Fig. 7*C* where the curves for the charge integral at various voltages were scaled up linearly by the size of the hyperpolarizing pulse. From this analysis (Fig. 7*C*) it was further concluded that the time course for charge movement *during* the pulse is similar to that *after* the pulse, and that the time courses are not significantly voltage-dependent (at least over the range −95 to −132·5 mV). The experiments of Fig. 7 strongly suggest, therefore, that the slow current transient behaves like a linear capacity current.

Dissected fibres with large currents without chemical treatment

If the hypothesis is correct, one might expect to see large potassium currents in fibres that were deliberately stretched during dissection, as this might also expose the paranodal region. Indeed, in several such tests we did find four such fibres with large potassium currents. All these four 'normal' fibres had one thing in common with those subjected to myelin-loosening treatment: all had an abnormally large apparent nodal capacity (35–96 pF). A family of nodal currents, and the associated leakage current,

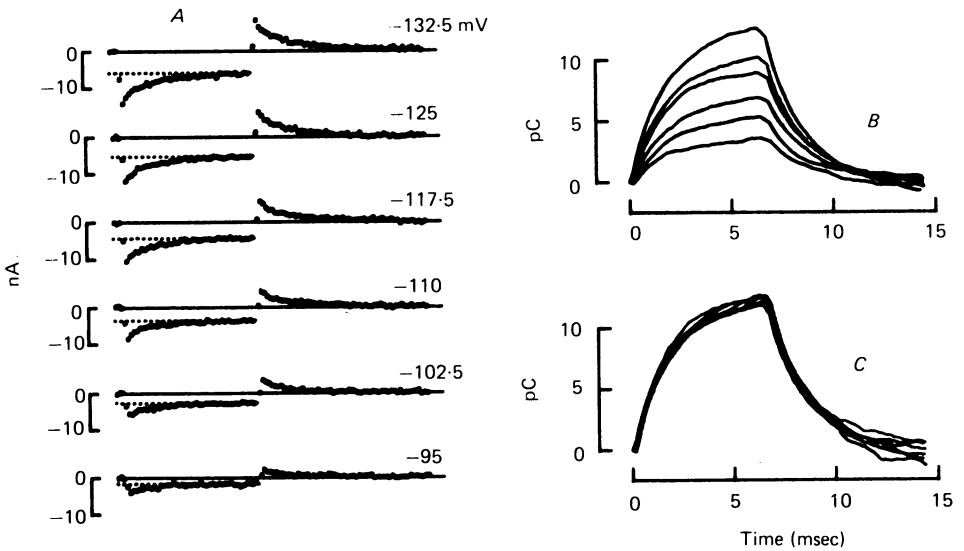

Fig. 7. The linear capacitative nature of the slow current transient. *A* shows a series of current responses to a series of hyperpolarizing pulses, each 6·6 msec long, to between −95 and −132·5 mV applied from a holding potential of −80 mV. The steady value to which the slow current settled during the pulse was obtained by fitting eqn. (1) to the last 2 msec portion of the current and the extrapolated steady value being shown by the dotted line. After subtraction of this steady value during the pulse, the current was integrated numerically from zero to 15 msec for each hyperpolarization; and the curves of the time course of the resulting charge movement are shown on the right (*B*). *C* was obtained from *B* by scaling each individual integrated curve in *B* by a factor (52·5/size of pulse), where 52·5 mV is the size of the largest hyperpolarization (to −132·5 mV). Current signals are sampled at intervals of 150 μsec through the entire time interval (0–15 msec) and the fast capacity transients are not shown.

from such a 'stretched' fibre are shown in Fig. 8*B*. Also shown (Fig. 8*A*) is a family of nodal currents from a different fibre, dissected from the same rabbit two hours earlier in which the usual care to avoid stretching was taken. Clearly, there is a marked difference in the size of the outward current in these two fibres; and it is equally clear that there is a marked corresponding difference in the capacity current transient. Thus there is a large slow capacitative transient in the fibre with the large outward current (Fig. 8*B*), which is absent in the fibre of Fig. 8*A* which has little or no outward current. This large capacity transient is similar to the slow capacity transients

produced by the treatment used in Fig. 5 to reveal large outward potassium current. We believe that the same hypothesis that was put forward to explain the production of large potassium current by the myelin-loosening treatment also explains the occurrence of large potassium current in such chemically untreated fibres: namely, the paranodal region is somehow damaged or exposed by mechanical stretching during dissection. The potassium currents in such fibres were, like the potassium currents revealed by treatment, only partially blocked by external TEA, which had a long wash-out time; but they were almost entirely blocked by internal application

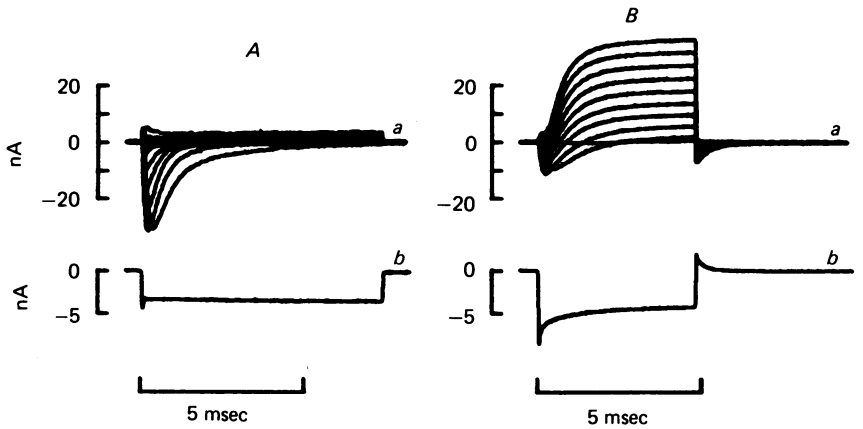

Fig. 8. Fibre with large potassium current before treatment. *A* shows a family of ionic currents in a normal rabbit node associated with a series of depolarizations from −65 mV to +70 mV in 15 mV increments. Note the usual absence of any substantial outward current. *Ba* shows a family of ionic currents in a different fibre of the same rabbit deliberately stretched during dissection. A large late outward current is seen in this fibre. The bottom single traces in *Ab* and *Bb* represent the leakage currents in response to hyperpolarizations to −125 mV. Clearly, the marked difference in the size of the late outward current in *Ba* is accompanied by a marked difference in the shape of the leakage in *Bb*; a slow current transient is prominent in *Bb* but not in *Ab*. Current signals were sampled every 30 μsec during the test pulse and every 150 μsec afterwards. Note that the time scale for the current after the pulse has thus been compressed fivefold compared with that used during the pulse. In addition, the fast capacity transients (first four to six points during the onset of the pulse) in *A* and *B* were sampled every 12 μsec. Temperature, 25 °C.

of TEA and Cs ions. Furthermore, the kinetic behaviour of the potassium current was similar to that of the current revealed by the myelin-loosening treatment. Thus, Fig. 9 shows that the time constant of the late current present in the 'stretched' fibres (○) was of the same order of magnitude as that produced by the chemical myelin-loosening treatment (●). The values for E_{Na} and for the late current (at +70 mV) for these 'stretched' fibres were 39·7 ± 4·3 mV ($n = 4$) and 37·4 ± 10 nA ($n = 4$) respectively; these values can be compared with the corresponding values of 52·3 ± 2·7 mV and 4·9 ± 0·7 nA obtained from the six fibres in Fig. 5 before treatment. Clearly, a 'stretched' fibre with a large late current had a lower E_{Na} (i.e. had a higher internal sodium concentration) than those with a small late current. This observation, coupled with the experiment of Fig. 1 which shows that deliberate chemical and

osmotic damage done to a fibre can markedly increase the late current with no immediate significant change in E_{Na}, rules out the possibility that the usual absence of substantial late current in dissected rabbit nodes (Chiu *et al.* 1979) is a result of block by sodium ions that have accumulated inside the node during dissection (Bergman, 1970).

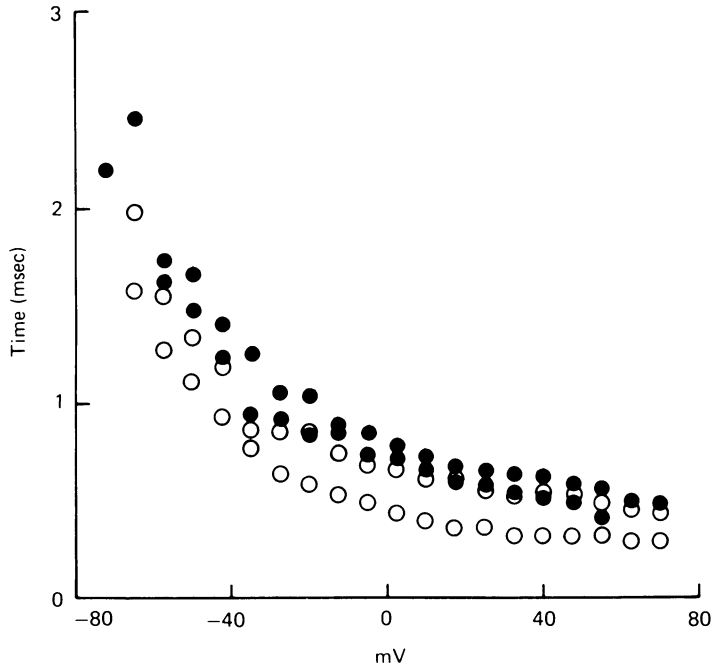

Fig. 9 Voltage-dependence of the time constant of the late outward current. ●, late currents revealed by lysolecithin and collagenase treatment (two fibres). ○, large late currents present in 'deliberately stretched' untreated fibres (two fibres). Temperature about 25 °C.

Outward current in the internode

Granted that potassium channels are to be found in the internodal region, are they located just in the paranode, or are they more generally distributed all along the internode? We attempted to answer this question by experiments in which only the internode was mounted in the voltage-clamp chamber. The myelin in the internodal region was then dissolved with lysolecithin, and the resultant demyelinated axon was voltage-clamped (i.e. there was no node in the *A* pool). Unfortunately, the experimental results were equivocal because the endpoint, once reached (after 30–90 min), was usually passed too rapidly for any ionic currents to be measured before the fibre became irretrievably damaged. However, currents could be measured in one of seven experiments in which the middle of the internode was dissolved, and in two of the six experiments where the demyelinated region was located as close to a node as possible without actually having a node in the *A*-pool (100–200 μm). These currents were always outward, and no inward sodium currents were seen. Clearly, more experiments are needed to settle this important point.

Computer simulation of voltage-clamp currents after acute demyelination

The effects of paranodal demyelination on the transient capacity currents and the ionic currents were examined in terms of the equivalent circuit shown in Fig. 10. In this analysis the axonal membrane was taken to be subdivided into a series of

elements each 2 μm long (the length of a normal nodal gap); the node (N) was located at the middle and an equal number of paranodal elements (PN) were coupled to its left and right in a parallel fashion. Each element had its associated membrane resistance (R_N, node; R_{PN}, paranode), capacity (C), sodium conductance (g_{Na}), and potassium conductance (g_K). Adjacent elements were connected by external series resistances (r_s) and internal axoplasmic resistance (r_a), with the node itself having

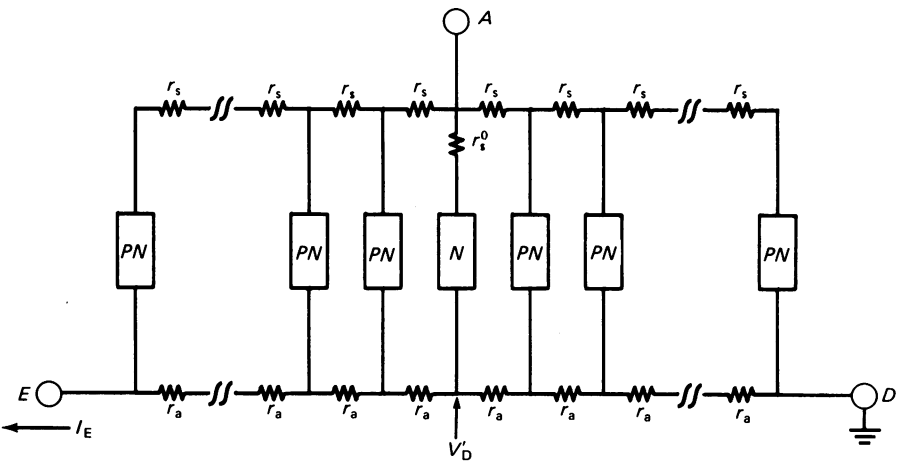

Fig. 10. Equivalent circuit for simulation of acute paranodal demyelination. A length of axon in the A-pool (see Chiu *et al.* 1979) is subdivided into a series of segments each 2 μm long. The node (N) is coupled on both sides to a symmetrical distribution of paranodal segments (PN) that are normally covered by myelin. Point D is held at virtual ground by the first amplifier (see Chiu *et al.* 1979), the command voltage is applied at point A (A-pool) and a current I_E flows at point E. r_s^0 is a small nodal series resistance and r_s represent the external longitudinal resistances along the length of each segment (2 μm) between the myelin and paranodal axonal membrane. r_a represents the longitudinal axoplasmic resistances between adjacent segments. V_D' is the internal potential at the node which is ideally zero when no current flow along the r_a on the right portion of the paranode. For a width of 2 μm for each segment, r_a would be about 0·02 MΩ (an average R_{ED} value of 7 MΩ is associated with a cut internodal length of about 700 μm in this study). r_s^0 is arbitrarily assumed to be 0·25 MΩ in the calculation. The capacity of each segment, C, is assumed to be 1·4 pF. r_a, $r^0{}_s$, and C are assumed to remain constant during demyelination. Acute paranodal demyelination is simulated by decreasing the three paranodal values for r_s immediately to the left and right of the node.

a small series resistance ($r^0{}_s$). Except for the node, all other elements were assumed to be normally covered by myelin, i.e., r_s is the resistance along 2 μm of periaxonal space. Acute demyelination was simulated by decreasing the first few r_s values immediately next to the node from some high initial values (i.e. to simulate the breaking of a tight paranodal-myelin seal), thus making the paranodal elements accessible to charging by a voltage step applied at A (Fig. 10). According to this model, the slow capacity transient after demyelination is a direct consequence of the complex charging process of the cable-like paranodal elements.

The solution for the current flow, I_E, in response to a voltage step applied at the A-pool (see Fig. 10) was obtained by numerical integration in steps of 0·2–0·5 μsec.

The slow capacity transient after demyelination was simulated in this model with 111 elements and the appropriate choice of parameters. As in Hille & Campbell (1976) the parameters were chosen by trial and error by comparing simulations with observations in the following way. All the paranodal membrane resistances R_{PN} were assumed to be identical. To simplify the choice of parameters further, the assumption

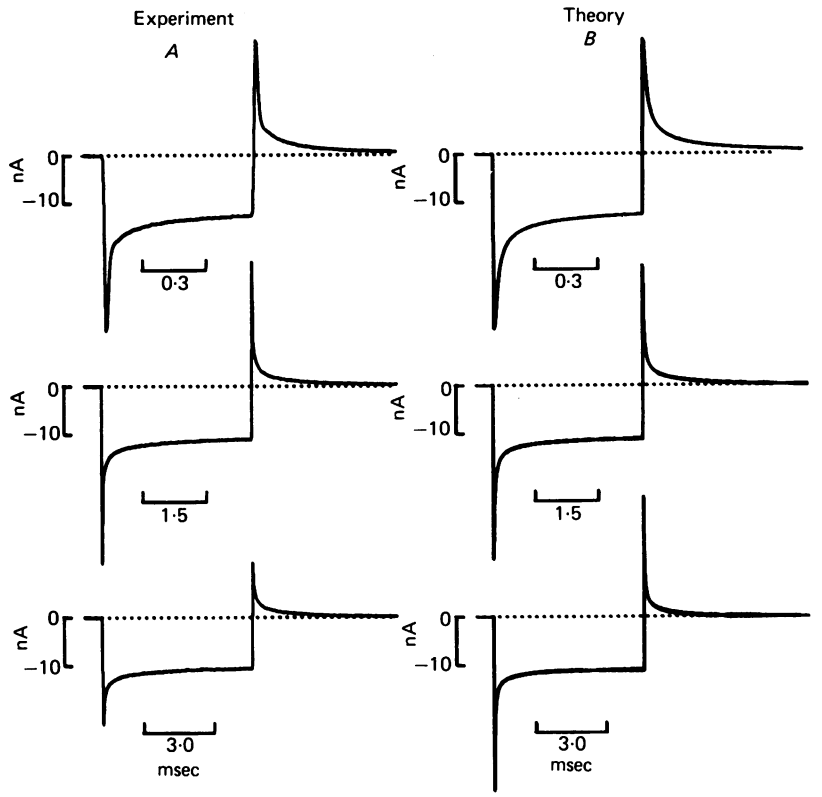

Fig. 11. Observed (*A*) and simulated (*B*) slow transient capacity currents. The observed leak and capacity currents in *A* were obtained with a hyperpolarizing step to −130 mV with the current signals sampled at progressively longer intervals; the sampling intervals (from top to bottom) being 5, 25 and 45 μsec respectively. *B* shows the corresponding theoretical simulations calculated from the equivalent circuit of Fig. 10 using 111 elements. The theoretical records were obtained by numerical integration in steps of 0·2–0·5 μsec (top to bottom) and were plotted every 5 μsec. The parameters used were : R_N, 5·36 MΩ; R_{PN}, 2000 MΩ; r_s, 0·95 MΩ and the potential at the *A*-pool (see Fig. 10) was assumed to approach its new steady level with a 6 μsec exponential time constant. The observed current signals (*A*) were filtered by a 33 kHz 4-pole Bessel filter in series with a RC filter with a time constant of 8 μsec.

was made that all paranodal r_s were equal after the paranodal-myelin seal was broken. Starting with an initial value for the nodal resistance R_N that corresponded roughly to the observed steady leakage, we found first a combination of R_{PN} and r_s that gave an appropriate slow transient in the simulation. R_N was then readjusted slightly to give the best final steady leak values. The experimentally observed slow capacity transient in Fig. 11 *A* (obtained at three different sweep speeds) was simulated in this

way in *B*. It should be noted that the simulation procedure revealed that the slow capacity transient could only be simulated on the basis of a membrane resistance for the paranode R_{PN} which is about 400 times larger than at the node R_N.

Using this model, we have also examined the effects of different types of axonal distribution of sodium and potassium channels on the voltage-clamp currents before and after demyelination. Fig. 12 shows such a calculation using 51 elements on the assumption that sodium channels were restricted to the node, and potassium channels were distributed uniformly over the entire paranode. Parameters were chosen to imitate the observed currents in Fig. 12*Aa*, *Ba*. Values for R_{PN} and r_s after demyelination were chosen as described above to give the corresponding appropriate slow capacity transient, and the control leakage before demyelination was simulated by increasing the three r_s values immediately to the left and right of the node to some high value. Panel *Ac* shows simulation of a family of ionic currents before demyelination and panel *Bc* shows the corresponding simulated ionic currents after demyelination. Panels *Ad* and *Bd* show the corresponding simulated leakage records.

The theoretical error in the voltage control at the node caused by demyelination was examined by calculating the internal potential at the node V'_D (see Fig. 10) for a depolarization of 67·5 mV. Whereas in the control the value of V'_D stayed virtually at ground level (Fig. 12*Ae*), after demyelination there was a clear deviation from zero (Fig. 12*Be*). The calculated deviation, however, was small ($< 0{\cdot}5$ mV), which is consistent with the observation that the current–voltge relation for the sodium currents showed practically no signs of poor voltage control after demyelination (Fig. 1). In contrast, the simulations showed that the potassium currents were definitely not under voltage control, as can be seen by calculating the axonal profile of the ratio of the size of the final voltage across each element to the size of the largest applied depolarization of 147·5 mV in the *A*-pool before (Fig. 12*Af*) and after (Fig. 12*Bf*) demyelination. Here, the solid curve shows the voltage profile and the dotted curves represent the final values of n^4 for the potassium current activated at each element (the peak of the curves corresponded to the position of the node). The potassium current in Fig. 12*Bc* is made up of contributions from a spectrum of paranodal elements each activated to various potential levels.

From the above values for r_s of 0·95–4·0 MΩ for simulation of the slow transient capacity current, the width of the periaxonal space between the myelin and the paranodal axon after demyelination can be estimated from the resistivity of the periaxonal fluid at 25 °C (assumed to be that of 160 mM-sodium chloride). For an axonal diameter of 14 μm, the values for r_s of 0·95–4·0 MΩ would correspond to a periaxonal space of width 75–300 Å. This value can be compared with a value of 150–200 Å for a normal periaxonal gap determined in electronmicroscopic studies (e.g. Berthold, 1978).

DISCUSSION

The present experiments on acutely demyelinated rabbit nerve suggest that potassium channels, which are not manifest in normal mammalian nodes (Horackova *et al.* 1968; Chiu *et al.* 1980; Brismar, 1980), do indeed exist in the normal internodal region. For the outward current revealed by the myelin-loosening treatment has,

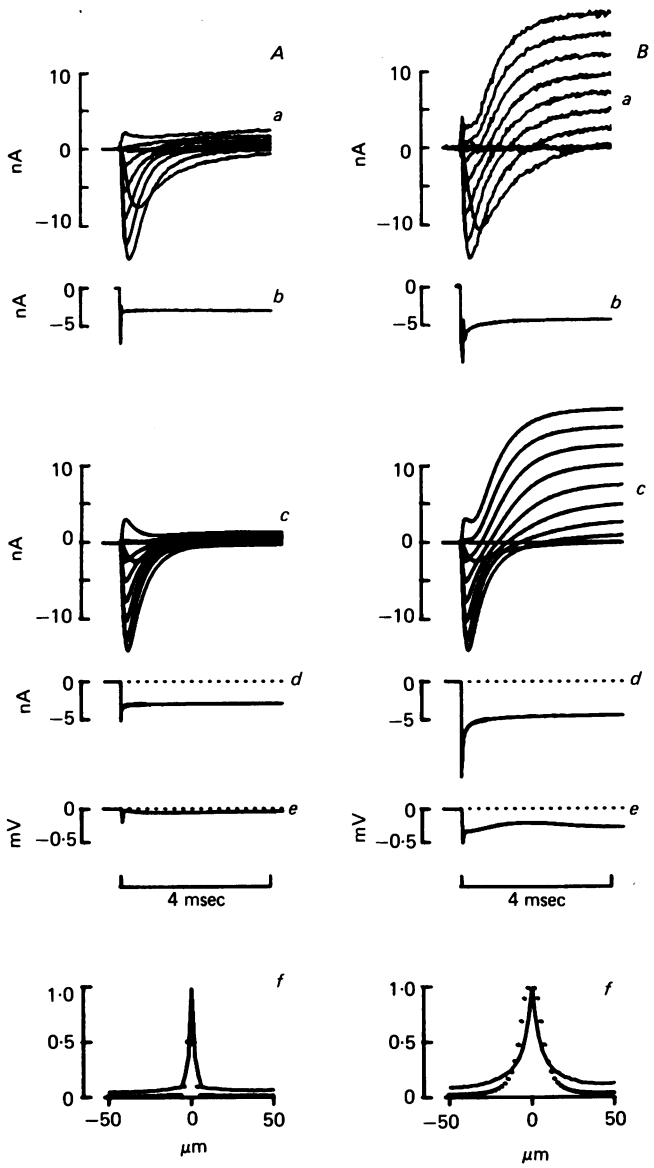

Fig. 12. Computer simulations of sodium and potassium currents before (*A*) and after (*B*) acute paranodal demyelination. The theoretical calculations shown in this Figure were made from the equivalent circuit in Fig. 10 using fifty-one elements (node at the 26th element) with the parameters deliberately chosen to match the experimentally observed current records *Aa*, *b* and *Ba*, *b* obtained from Chiu & Ritchie (1980*a*). The record *Ac* shows simulation of a normal family of voltage clamp currents for a rabbit node initially held at −80 mV and then depolarized to various test potentials in the range −72·5 mV to 62·5 mV in 15 mV increments. The passive parameters used were: R_N, 17·2 MΩ; R_{PN}, 1800 MΩ; the first three r_s values immediately to the left and right of the node were each 75 MΩ, and all other r_s, 4 MΩ. The active parameters were: nodal $g_{Na} = 0{\cdot}41$ μS and $g_K = 0$; and for all the paranodal elements $g_{Na} = 0$ and $g_K = 0{\cdot}034$ μS. The currents were corrected for a linear leakage using the leak and capacity currents calculated for a step

qualitatively, several of the important characteristics of a potassium current: it is sensitive to external potassium in the way expected (the reversal potential becoming more positive as $[K]_o$ increases): the tail currents become more prominent as the duration of the voltage-clamp test pulse is increased; the kinetic behaviour is similar to that of the known potassium current in the frog; and finally, it is sensitive to internal TEA and caesium.

In a normal myelinated nerve, a gap of 150–200 Å is present between the internodal axon and the surounding myelin except at the paranodal region immediately next to the node where the myelin loops terminate to form a tight seal 2–4 μm long around the axon and are separated from the axonal membrane by a space 20–30 Å thick containing a quite complex morphology (see Berthold, 1978; Schnapp & Mugnaini, 1978). This tight seal may well be broken quite early during the demyelination treatments thus allowing electrical communication between the periaxonal space and the external bathing fluid. There is, at present, no microscopic evidence for this. But there is good electrophysiological evidence for such a disruption, namely the appearance of the slow capacity current which is taken to reflect charging of the now accessible paranodal axon. This interpretation is strengthened by two factors. Firstly, a simple cable-like model (Fig. 10) could be used successfully to simulate the slow capacity current with a reasonable choice of parameters. Secondly, the parameters used in the simulation of the slow capacity current (i.e. r_s values ranging 0·95–4·0 MΩ) yielded an estimate for a width of 75–300 Å for the periaxonal space, which is the same order of magnitude as the values of 150–200 Å found electronmicroscopically (Berthold, 1978). This calculation suggests that the demyelinating treatment used (and possibly the deliberate stretching of the fibres) need not produce a drastic structural disruption with a complete lifting of the myelin; but rather there may well be just a relatively discrete breaking or interruption of the myelin-paranodal seal extending over no more than a few microns. Diffusion of ions would still be slow from the external medium into and along the periaxonal space from this opened end, which may well explain why the block of potassium current by external TEA is slow and incomplete compared with the fast block of the sodium current by external TTX.

---

hyperpolarization of −45 mV as shown in *Ad*. *Bc* shows simulation of the effect of acute paranodal demyelination on the ionic current. The simulations were made by changing only two of the passive parameters used in *Ac*: the first three r_s values immediately to the left and right of the node were decreased from 75 MΩ to 4 MΩ thus making all r_s values uniform at 4 MΩ; and R_N was changed from 17·2 MΩ to 12·5 MΩ. *Ae* and *Be* show the time dependence of the internal potential V_D' (see Fig. 10) associated with a test depolarization of 67·5 mV before (*Ae*) and after (*Be*) demyelination. The solid curves in *Af* and *Bf* show the longitudinal axonal profile of the ratio of the size of the final voltage across each element to the size of a test depolarization of 142·5 mV applied at the *A*-pool before (*Af*) and after (*Bf*) demyelination. Also shown in the same plots (dotted curves) are the profiles of the final values of n^4 for the potassium current activated in each paranodal element. The calibration of the axonal distance assumed a segment width of 2 μm; the node is positioned at 0 with the negative and positive portions of the axis representing the left and right paranodes respectively. Rate constants for the sodium currents were those of Chiu *et al.* (1979) arbitrarily scaled by a factor of 2 to allow for temperature differences. Rate constants for potassium currents were taken from Hille (1971) for frog nodes scaled by a factor of 1·6 to make the simulated potassium currents match the observations.

No marked change (of probably not more than 5 %) in the size of the sodium current was observed at the critical moment of demyelination when the late current showed a dramatic increase (Fig. 12*Ba*); nor was the current–voltage relationship changed. Theoretical calculations showed that this is consistent (at least for the extent of demyelination achieved in the experiment of Fig. 12) with an axonal distribution in which sodium channels are restricted mostly to the nodal region. If the sodium channels are indeed so distributed, demyelination up to a certain extent (as in Fig. 12) will cause only small errors in their voltage control and no significant changes in current size will be observed. Given that the acute demyelinating treatments may have a direct effect on the axonal membrane, the present voltage-clamp finding on the sodium current is thus consistent with the saxitoxin labelling experiments of Ritchie & Rogart (1977) who concluded that the bulk of the sodium channels were located in the nodal membrane.

What is the function of this complementary distribution of channels in mammalian myelinated nerve, the sodium channels being located largely in the node and the potassium channels in the internode? It is easy to understand why the sodium channels might have to be largely restricted to the nodes (where they are needed to generate the conducted impulse) and virtually absent from the internodal region (where they are not required) – although they may be present there in small quantities, or may appear there after chronic demyelination, and so support the continuous conduction noted by Bostock & Sears (1978). The reason for the complementary distribution of potassium channels is less obvious. One reason for their being absent from the node of Ranvier is that there may be no room for them. For the fast speed of conduction for which myelinated fibres are specialized requires a high nodal sodium conductance, i.e. a high density of sodium channels. Gating current measurements (Chiu, 1980) suggest that in both frog and rabbit fibres there are about 100,000 sodium channels per node; and saxitoxin binding studies suggest even more in the rabbit (Ritchie & Rogart, 1977). Clearly, the lack of potassium channels leaves room for more sodium channels to be packed into the restricted nodal area. Furthermore, the absence of potassium channels from the node will have the additional advantage of allowing more frequent excitation for two reasons. Firstly, if the increase in potassium conductance following an action potential were very prolonged, as in squid nerve, there would be a temporary rise in the threshold current required to excite the fibre again; and secondly potassium currents might lead to an accumulation of potassium in the nodal periaxonal space. The ability of the node to generate an impulse soon after a preceding one would thus again be compromised. On this basis there would clearly be no need to remove potassium channels from the internodal axonal membrane; and this may well be the reason why they persist there.

However, it is interesting to speculate that they do have a positive role to play. In squid giant axons and many other conducting tissues the onset of repolarization is brought about, at least in part, by the delayed outward potassium current thus prolonging the effective refractory period. This factor plays no role in rabbit nerve (Chiu *et al.* 1979) and repolarization must follow the inactivation of the sodium current. If (as expected on the basis of Hodgkin–Huxley kinetics) recovery from inactivation were as fast as its onset, which is 2–3 times faster in the rabbit than in the frog node of the same diameter and at the same temperature at a membrane potential of −50 mV and faster still at the normal resting potential, the action potential would be quite short. In fact Chiu *et al.* (1979) calculated on the basis of Hodgkin–Huxley kinetics that the action

potential in the rabbit is of slightly shorter duration than in the frog. Thus soon after the membrane potential has returned to its resting value, the mammalian node is ready to respond to the next impulse. However, one danger of tuning the system so finely is that any persisting depolarization in a patch of tissue near the node may re-excite the node, and cause repetitive firing after a single impulse, in a way analogous to the re-entrant and ectopic phenomena that are well known in cardiac muscle. Such phenomena require the presence of delayed or slowly developing responses. One possible locus for such phenomena is the paranodal region. The sodium channels are located mainly in the nodal membrane, with very few, if any, in the internodal axonal membrane. It is unlikely, however, that the demarcation between nodal and internodal membrane is absolutely sharp: rather, sodium channels are probably present to some extent in the paranode, but with an ever decreasing density at increasing distances from the node proper. It is possible, therefore, that a delayed slowly developing response occurs in the node/paranode junction, delayed because of the high series resistance of the external path between the node proper and some paranodal patch of membrane, and slowly developing because of the relative paucity of sodium channels in this area. Thus, since the sodium channels in the mammalian node recover so rapidly from inactivation, they are at risk of being re-excited by this persisting depolarization. On this basis the function of the potassium channels in the paranodal region would be to dampen the paranodal response.

This hypothesis (that the function of the paranodal potassium channels is to prevent spurious nodal re-excitation) is at the moment quite speculative, although preliminary computer simulation studies based on a high series resistance in the region of the paranodal seal followed by a much lower series resistance along the rest of the internode, and on high axonal membrane resistances except at the node, show that such re-excitation is quite feasible. Too little, however, is known about the electrical parameters of the internode to warrant detailed speculation. It is interesting, however, that the hypothesis is in fact consistent with experimental findings in other tissues, where potassium channels seem to protect against repetitive firing. For example, frog sensory fibres, which have less prominent potassium currents and a greater sensitivity to TEA (for references see Stämpfli & Hille, 1976), are more liable to fire repetitively in response to a constant stimulating current than frog motor fibres. Furthermore, as Bergman, Nonner & Stämpfli (1968) point out, frog nodes in low-calcium solutions practically never exhibit spontaneous firing; but they do if TEA is added. Finally, Kyrlov & Makovsky (1978) have recently presented evidence that a slowly developing increase in potassium conductance is responsible for the phenomenon of spike frequency adaptation in amphibian sensory fibres.

This stabilizing effect of potassium channels might also be important in pathophysiological situations. Simply uncovering potassium channels might be expected to stabilize a membrane. But pathological demyelination is clearly more complex; and, in fact, chronically demyelinated fibres (Howe, Calvin & Loeser, 1976) and the hypomyelinated fibres studied by Rasminsky (1978) are hyperexcitable. For example, they show spontaneous generation of impulses and repetitive firing in response to a single impulse. Furthermore, the paraesthesias and the paroxysmal symptoms of multiple sclerosis may well reflect spontaneous firing at demyelinating nodes (see Rasminsky, 1978). One function of the potassium channels in the internodal region, particularly in the paranodal region, therefore, might be to provide a chemical voltage-clamp in the paranodal area and hence offset the hyperexcitability of the damaged fibre by restricting the degree to which a partially demyelinated patch of nerve can exhibit a slow regenerative response which might subsequently re-excite other areas of the fibre.

This work was supported in part by a grant RG 1152 from the U.S. National Multiple Sclerosis Society and by a grant NS 12327 from the U.S.P.H.S.

REFERENCES

BERGMAN, C. (1970). Increase of sodium concentration near the inner surface of the nodal membrane. *Pflügers Arch.* **317**, 287–302.

BERGMAN, C., NONNER, W. & STÄMPFLI, R. (1968). Sustained spontaneous activity of Ranvier nodes induced by the combined actions of TEA and lack of calcium. *Pflügers Arch.* **302**, 24–37.

BERTHOLD, C-H. (1978). Morphology of normal peripheral axons. In *Physiology and Pathology of Axons*, ed. WAXMAN, S. G., pp. 3–63. New York: Raven.

BOSTOCK, H. & SEARS, T. A. (1978). The internodal axon membrane: electrical excitability and continuous conduction in segmental demyelination. *J. Physiol.* **280**, 273–301.

BRISMAR, T. (1979). Potential clamp analysis on myelinated nerve fibres from alloxan diabetic rats. *Acta physiol. scand.* **105**, 384–386.

BRISMAR, T. (1980). Potential clamp analysis of membrane currents in rat myelinated nerve fibres. *J. Physiol.* **298**, 171–184.

CHIU, S. Y. (1980). Asymmetry currents in the mammalian myelinated nerve. *J. Physiol.* **309**, 499–519.

CHIU, S. Y. & RITCHIE, J. M. (1980*a*). Potassium channels in nodal and internodal axonal membrane of mammalian myelinated fibres. *Nature, Lond.* **284**, 170–171.

CHIU, S. Y. & RITCHIE, J. M. (1980*b*). Potassium channels in the paranodal region of acutely demyelinated voltage-clamped mammalian myelinated nerve. *J. Physiol.* **305**, 61–62*P*.

CHIU, S. Y., RITCHIE, J. M., ROGART, R. B. & STAGG, D. (1979). A quantitative description of membrane currents in rabbit myelinated nerve. *J. Physiol.* **292**, 149–166.

COLE, K. S. & MOORE, J. W. (1960). Potassium ion current in the squid giant axon: dynamic characteristic. *Biophys. J.* **1**, 1–14.

FRANKENHAEUSER, B. & HODGKIN, A. L. (1956). The after effects of impulses in the giant nerve fibres of *Loligo*. *J. Physiol.* **131**, 341–376.

HALL, S. (1972). The effect of injections of lysophosphatidyl choline into white matter of the adult mouse spinal cord. *J. cell Sci.* **10**, 535–546.

HILLE, B. (1967). The selective inhibition of delayed potassium current in nerve by tetraethylammonium ion. *J. gen. Physiol.* **50**, 1287–1302.

HILLE, B. (1971). Voltage clamp studies on myelinated nerve fibers. In *Biophysics and Physiology of Excitable Membranes*, ed. ADELMAN, W. J., pp. 230–246. New York: Van Nostrand Reinhold.

HILLE, B. & CAMPBELL, D. (1976). An improved vaseline gap voltage clamp for skeletal muscle fibres. *J. gen. Physiol.* **67**, 265–293.

HODGKIN, A. L. & HOROWICZ, P. (1959). The influence of potassium and chloride ions on the membrane potential of single muscle fibres. *J. Physiol.* **148**, 127–160.

HODGKIN, A. L. & HUXLEY, A. F. (1952). A quantitative description of membrane current and its application to conduction and excitation in nerve. *J. Physiol.* **177**, 500–544.

HODGKIN, A. L., HUXLEY, A. F. & KATZ, B. (1952). Measurement of current–voltage relations in the membrane of the giant axon of *Loligo*. *J. Physiol.* **116**, 424–448.

HORACKOVA, M., NONNER, W. & STÄMPFLI, R. (1968). Action potentials and voltage clamp currents of single rat Ranvier nodes. *Proc. int. Union Physiol. Sci.* **7**, 198.

HOWE, J. F., CALVIN, W. H. & LOESER, J. D. (1976). Impulses reflected from dorsal root ganglia and from focal nerve injuries. *Brain Res.* **116**, 139–144.

KEYNES, R. D. & KIMURA, J. E. (1980). The effect of starting potential on activation of the ionic conductances in the squid giant axon. *J. Physiol.* **308**, 17*P*.

KOPPENHÖFER, E. & VOGEL, W. (1968). Effects of tetrodotoxin and tetraethylammonium chloride on the inside of the nodal membrane of *Xenopus laevis*. *Pflügers Arch.* **313**, 361.

KYRLOV, B. V. & MAKOVSKY, V. S. (1978). Spike frequency adaptation in amphibian sensory fibres is probably due to slow K channels. *Nature, Lond.* **275**, 549–551.

MOBLEY, B. A. & PAGE, E. (1971). The effect of potassium and chloride ions on the volume and membrane potential of single barnacle muscle cells. *J. Physiol.* **215**, 49–70.

RASMINSKY, M. (1978). Physiology of conduction in demyelinated axons. In *Physiology and Pathobiology of Axons*, ed. WAXMAN, S. G., pp. 361–376. New York: Raven.

RITCHIE, J. M. & ROGART, R. B. (1977). The density of sodium channels in mammalian myelinated nerve fibers and the nature of the axonal membrane under the myelin sheath. *Proc. natn. Acad. Sci. U.S.A.* **74**, 211–215.

SCHNAPP, B. & MUGNAINI, E. (1978). Membrane architecture of myelinated fibers as seen by freeze-fracture. In *Physiology and Pathobiology of Axons*, ed. WAXMAN, S. G., pp. 83–123. New York: Raven.

SHERRATT, R. M., BOSTOCK, H. & SEARS, T. A. (1980). Effects of 4-aminopyridine on normal and demyelinated nerve fibres. *Nature, Lond.* **283**, 570–572.

SMITH, M. E. & BENJAMINS, J. A. (1977). Model systems for study of perturbation of myelin metabolism. In *Myelin*, ed. MORELL, P., pp. 447–488. New York: Plenum.

STÄMPFLI, R. & HILLE, B. (1976). Electrophysiology of the peripheral myelinated nerve. In *Frog Neurobiology*, ed. LLINAS, R. & PRECHT, W., pp. 1–32. Berlin: Springer-Verlag.